DOI: 10.1002/chem.200601224

One-Step Synthesis of Large-Aspect-Ratio Single-Crystalline Gold Nanorods by Using CTPAB and CTBAB Surfactants**

Xiaoshan Kou,[a] Shuzhuo Zhang,[a, b] Chia-Kuang Tsung,[a, c] Zhi Yang,[a] Man Hau Yeung,[a] Galen D. Stucky,[c] Lingdong Sun,[b] Jianfang Wang,*[a] and Chunhua Yan[b]

Abstract: Gold nanorods were prepared in high yields by using a one-step seed-mediated process in aqueous cetyltripropylammonium bromide (CTPAB) and cetyltributylammonium bromide (CTBAB) solutions in the presence of silver nitrate. The diameters of the nanorods range from 3 to 11 nm, their lengths are in the range of 15 to 350 nm, and their aspect ratios are in the range of 2 to 70. The diameters of the Au nanorods obtained from one growth batch in CTPAB solutions decrease as their lengths increase, and their volumes decrease as the aspect ratios increase. The diameters of the Au nanorods obtained from one growth batch in CTBAB solutions first decrease and then slightly increase as their lengths increase, and their volumes increase as the aspect ratios increase. These Au nanorods are single-crystalline and are seen to be oriented in either the [100] or [110] direction under transmission electron microscopy imaging, irrespective of their sizes. To the best of our knowledge, this is the first report of the preparation by using wet-chemistry methods of single-crystalline Au nanorods with aspect ratios larger than 15.

Keywords: gold · micelles · nanorods · surface plasmon resonance · surfactants

Introduction

Gold nanorods exhibit two surface plasmon resonance modes. One is the longitudinal surface plasmon mode that is associated with electron oscillations parallel to the rod-length axis, and the other is the transverse surface plasmon mode that is associated with electron oscillations perpendicular to the rod-length axis. Both experimental[1] and theoretical[2] studies have shown there is a high linear dependence of the longitudinal plasmon wavelength (LPW) of Au nanorods upon their length-to-diameter aspect ratio. A slight variation in the aspect ratio of Au nanorods can induce distinct color changes. Gold nanorods have, therefore, received attention because of their potential applications in photonics, optoelectronics, and biotechnology. For example, for biotechnological applications, the LPW of Au nanorods can be readily tuned to the near-infrared (NIR) spectral region to obtain optimal penetration depths into biological tissues.[3] Gold nanostructures also possess additional attractive features, such as chemical stability, biological compatibility, and rich surface-functionalization chemistry. Furthermore, light emitted from or scattered off Au nanorods is strongly polarized, making these an ideal orientation probe.[4] Owing to these attractive properties, Au nanorods have been demonstrated to function as scattering[5] and two-photon luminescent chromophores[6] for biological imaging, biological sensors,[7,8] carriers for drug delivery,[9] and therapeutic agents for photothermal cancer treatment.[5]

Gold nanorods have been grown in the presence of micelle-forming cationic surfactants by electrolysis at cathodic potentials,[10] by UV-light irradiation,[11] or by chemical reduction of Au(III) complex ions.[12] With regard to the latter method, it has been shown that a seed-mediated growth

[a] X. Kou, S. Zhang, C.-K. Tsung, Dr. Z. Yang, M. H. Yeung, Prof. J. Wang
Department of Physics, Chinese University of Hong Kong
Shatin, Hong Kong (China)
Fax: (+852) 2603-5204
E-mail: jfwang@phy.cuhk.edu.hk

[b] S. Zhang, Prof. L. Sun, Prof. C. Yan
State Key Lab of Rare Earth Materials Chemistry and Applications
Peking University, Beijing 100871 (China)

[c] C.-K. Tsung, Prof. G. D. Stucky
Department of Chemistry and Biochemistry
University of California, Santa Barbara, California 93106 (USA)

[**] CTPAB = cetyltripropylammonium bromide, CTBAB = cetyltributylammonium bromide.

Supporting information for this article is available on the WWW under http://www.chemeurj.org/ or from the author.

under mildly reducing conditions can produce multiply twinned Au nanorods with exquisite control over size and shape. It has been demonstrated further that the addition of $AgNO_3$ during the seed-mediated growth can produce single-crystalline Au nanorods in one step in nearly quantitative yields.[13–15] However, the aspect ratios and LPWs of the Au nanorods produced by using the one-step seed-mediated process in the presence of $AgNO_3$ are limited to below 13 and 1700 nm, respectively, after consideration of the extinction-peak broadening.[13] To the best of our knowledge, the preparation of single-crystalline Au nanorods with aspect ratios greater than 15 has not yet been reported. To date, only multiply twinned Au nanorods with aspect ratios larger than 15 have been produced in relatively low yields by using a multistep seed-mediated growth process.[12,16,17] Appropriate methods for the preparation of large-aspect-ratio Au nanorods are strongly desirable to extend the potential photonic and optoelectronic applications of Au nanorods to the infrared spectral region. Large-aspect-ratio Au nanorods could also function as interconnectors and contact electrodes, providing opportunities for the assembly with semiconductor nanowires into integrated electronic and photonic circuits by chemical and/or biological means.[8,18]

The most widely used cationic surfactant for the growth of Au nanorods is cetyltrimethylammonium bromide (CTAB). It is generally believed that CTAB plays two roles during the growth of Au nanorods in aqueous solutions. First, CTAB surfactants adsorb onto Au nanorods in a bilayer fashion with the trimethylammonium headgroups of one monolayer facing the nanorod surface.[19] CTAB adsorption makes Au nanorods positively charged and, therefore, stabilizes them in aqueous growth solutions. The growth of Au nanorods is probably governed by the preferential adsorption of CTAB surfactants onto different surfaces. Second, CTAB surfactants form micelles in aqueous solutions. The negatively charged complex ions of Au(III) and Au(I) bind to the positively charged headgroups around the micelles to establish an association–dissociation equilibrium. This binding between the complex ions and the micelles could alter the kinetics and energetics of the redox reaction and, therefore, the growth of Au nanorods. Previous experiments have investigated the effect of the tail length of alkyltrimethylammonium surfactants on the growth of Au nanorods,[16] however, little attention has been paid to the possible effect of the surfactant headgroup, even though the headgroup plays an important role in the micellization behavior of cationic surfactants.

We have reported recently the growth of Au nanorods in the aqueous solutions of cetyltriethylammonium bromide (CTEAB) surfactant by using the seed-mediated process in the presence of $AgNO_3$.[20] The maximum aspect ratio and LPW of the Au nanorods obtained in one-step growth are 11 and 1500 nm, respectively, after consideration of the extinction-peak broadening. By comparison, the maximum aspect ratio and LPW of the Au nanorods obtained in aqueous CTAB solutions under similar growth conditions without the use of cosurfactants are 5 and 900 nm, respectively.[14] The Au nanorods grown by using CTEAB, which has a larger headgroup, have larger aspect ratios. On the basis of this result, we expect that the growth by using surfactants of even larger headgroups under similar conditions might produce Au nanorods of even larger aspect ratios. Herein, we report the one-step growth of Au nanorods in aqueous cetyltripropylammonium bromide (CTPAB) and cetyltributylammonium bromide (CTBAB) solutions by using the seed-mediated process in the presence of $AgNO_3$. The Au nanorods have diameters from 3 to 11 nm, lengths from 15 to 350 nm, and aspect ratios from 2 to 70. They are single-crystalline and are seen to be oriented in either the [100] or [110] direction under transmission electron microscopy (TEM) imaging, irrespective of their sizes. Size measurements show that the volume of the individual nanorods obtained from one growth batch in CTPAB solutions decreases as the aspect ratio increases, and that the volume of the nanorods obtained from CTBAB solutions increases as the aspect ratio increases.

Results and Discussion

Synthesis of gold nanorods: The procedure we used for the growth of Au nanorods in aqueous CTPAB and CTBAB solutions is similar to those used previously by others for the growth of Au nanorods in CTAB solutions.[14,21] The presence of $AgNO_3$ improves significantly the yields of Au nanorods and leads to the production of single-crystalline Au nanorods by stabilizing high-energy side facets. The types of Au nanoparticle seeds used during growth also play an important role.[22] We used four types of seeds that were stabilized with CTAB, CTEAB, CTPAB, and CTBAB surfactants. We found that the CTAB- and CTEAB-stabilized seeds give higher yields of Au nanorods than the CTPAB- and CTBAB-stabilized seeds for the growth in CTPAB and CTBAB solutions (Table 1, Figures 1, 2, and Supporting Information Figures S1–S5), presumably due to their difference in stability. The CTAB- and CTEAB-stabilized seed solutions kept in a water bath maintained at room tempera-

Table 1. Approximate times required for the complete growth, and the estimated yields, of gold nanorods under different conditions.

Seed[a]	Surfactant[b]	Growth time[c]	Yield of nanorods[d]
seed III	CTPAB (0.1 M)	3 d	20%
seed III	CTPAB (0.01 M)	4 h	60%
seed II	CTPAB (0.01 M)	4 h	90%
seed I	CTPAB (0.01 M)	4 h	90%
seed IV	CTBAB (0.01 M)	4 d	10%
seed II	CTBAB (0.01 M)	4 d	90%
seed I	CTBAB (0.01 M)	4 d	60%

[a] Seed I: CTAB-stabilized seeds; seed II: CTEAB-stabilized seeds; seed III: CTPAB-stabilized seeds; seed IV: CTBAB-stabilized seeds. [b] Surfactants and concentrations used in aqueous growth solutions. [c] Approximate time required for complete growth was estimated from time-dependent extinction spectra. [d] Yields of Au nanorods were estimated according to their low-magnification TEM images and extinction spectra.

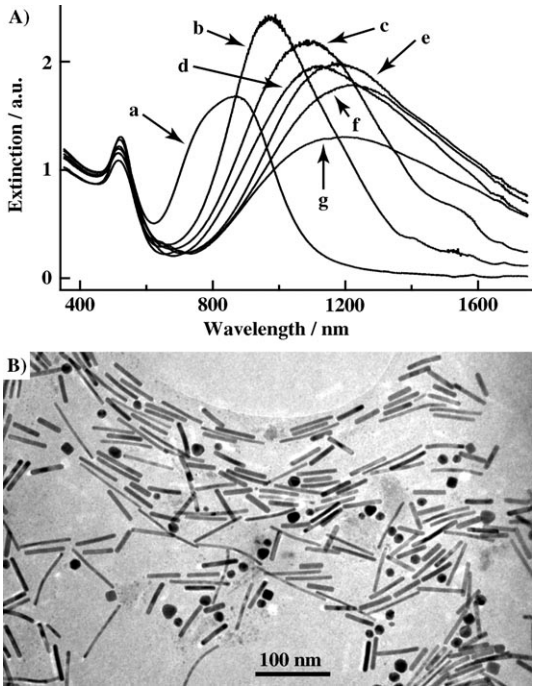

Figure 1. A) Extinction spectra of Au nanorods grown in CTPAB solutions (0.01 M) by using various volumes of the CTEAB-stabilized seed solution: a) 0.500, b) 0.300, c) 0.200, d) 0.150, e) 0.075, f) 0.050, and g) 0.030 mL. The spectra were recorded one day after addition of the seed solution. B) TEM image of nanorods grown in a CTPAB solution (0.01 M) by using the CTEAB-stabilized seed solution (0.150 mL).

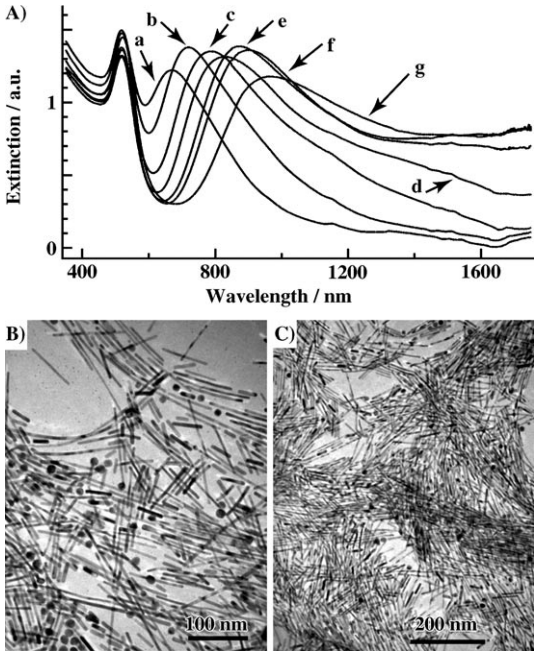

Figure 2. A) Extinction spectra of Au nanorods grown in CTBAB solutions (0.01 M) by using various volumes of the CTEAB-stabilized seed solution: a) 0.500, b) 0.300, c) 0.200, d) 0.150, e) 0.100, f) 0.075, and g) 0.050 mL. The spectra were recorded at least four days after addition of the seed solution. B), C) TEM images of nanorods grown in a CTBAB solution (0.01 M) by using the CTEAB-stabilized seed solution (0.100 mL). The two images were recorded at different locations on the same TEM grid. The aspect ratios of many of the nanorods shown in B) and C) are larger than 15.

ture remain brown-yellow for more than one day after preparation, whereas the CTPAB- and CTBAB-stabilized seed solutions change from brown-yellow to light-red $\approx$2 h and $\approx$30 min, respectively, after preparation.

We also found that the growth in CTPAB and CTBAB solutions at a concentration of 0.01 M gives high yields of Au nanorods (Table 1). The growth in CTPAB solutions at a concentration of 0.1 M is slow, requiring more than three days, and gives lower yields of Au nanorods. CTBAB has a lower solubility in water than CTPAB. Phase separation occurs at room temperature in the CTBAB solutions that were made at 80 °C at a concentration of 0.1 M. Therefore, we focused on the growth of Au nanorods in CTPAB and CTBAB solutions at a concentration of 0.01 M.

Figure 1A shows the extinction spectra of the Au nanorods grown in CTPAB solutions (0.01 M) with varying amounts of the CTEAB-stabilized seed solution. Each spectrum exhibits two surface plasmon-related extinction peaks. The longitudinal plasmon peaks are much stronger and broader than the transverse plasmon peaks, indicating that Au nanorods are the dominant growth product. As the amount of seed solution decreased, the LPW of the nanorods red-shifted, the longitudinal plasmon peak became broader, and the tail at the longer-wavelength side extended further, finally beyond the upper wavelength limit of our spectrophotometer. The estimated maximum LPW of these Au nanorods is 2000 nm. By comparison, the maximum LPWs of the Au nanorods grown in CTAB and CTEAB solutions in one step are 900 and 1500 nm, respectively.[14,20] Figure 1B shows a typical TEM image of the Au nanorods grown with the CTEAB-stabilized seed solution (0.150 mL, Figure 1A, curve d). The growth gives high yields of Au nanorods, together with a small proportion of roughly spherical particles. Each nanorod has a uniform diameter along its length axis. The length and diameter distributions of the nanorods are relatively broad, which is consistent with their broad longitudinal plasmon peaks.

Figure 2A shows the extinction spectra of the Au nanorods produced in CTBAB solutions (0.01 M) with varying amounts of the CTEAB-stabilized seed solution. As the amount of the seed solution decreased, the LPW of the nanorods red-shifted, and the tail at the longer-wavelength side extended further. For the Au nanorods grown with 0.100 mL (Figure 2A, curve e), 0.075 mL (Figure 2A, curve f), and 0.050 mL (Figure 2A, curve g) of the CTEAB-stabilized seed solution, the longitudinal plasmon peaks stay almost constant at a significant extinction value above $\approx$1200 nm and extend without decaying beyond the detection limit of our spectrophotometer. These nondecaying tails indicate the presence of a significant proportion of Au nanorods that have aspect ratios larger than 15. In addition, although the longitudinal plasmon peak height is comparable to the transverse plasmon peak height, the integrated area of the former is much larger than that of the latter. The

larger areas of the longitudinal plasmon peaks suggest the presence of high yields of Au nanorods that are polydisperse in aspect ratio.

Figure 2B shows the typical TEM image of the Au nanorods grown in CTBAB solutions (0.01 M) with the CTEAB-stabilized seed solution (0.100 mL, Figure 2A, curve e). The dominant growth product is Au nanorods, which are polydisperse in length. Only very few roughly spherical particles are present. Figure 2C shows the TEM image that was recorded at a different location on the same TEM grid as the image shown in Figure 2B. Gold nanorods of relatively uniform length are densely packed together and a large number of them have aspect ratios greater than 15. TEM imaging reveals that about half of the entire grid area is covered by densely packed Au nanorods that have aspect ratios greater than 15. In addition, no separation steps were involved in the preparation of the samples for TEM observation during our experiments.

The CTAB and CTEAB surfactant concentration used in previous high-yield growth of Au nanorods was 0.1 M.[14,20] The optimal CTPAB and CTBAB concentration that gives high yields of Au nanorods in our experiments was 0.01 M. Control growth experiments were carried out in both CTAB and CTEAB solutions at a concentration of 0.01 M. Extinction spectra (Supporting Information Figures S6 and S7) show that the yields of Au nanorods are lower than those from the growth in CTAB and CTEAB solutions at a concentration of 0.1 M. The Au nanorods obtained from the growth at the two different surfactant concentrations have comparable aspect ratios. These results indicate that in our experiments the growth of Au nanorods with large aspect ratios is due to the inherent nature of CTPAB and CTBAB surfactants, and not to the different surfactant concentrations.

Temporal evolution of the extinction spectra was monitored during growth to determine the approximate time that is required for the complete growth of Au nanorods in CTPAB and CTBAB solutions. Figure 3A and B show the time-dependent extinction spectra of nanorod growth in CTPAB (0.01 M) and CTBAB (0.01 M) solutions, respectively, by using the CTEAB-stabilized seeds. During growth, the LPW red-shifts over time, and the transverse plasmon wavelength stays constant. Both the transverse and longitudinal plasmon peaks increase in intensity over time. It takes $\approx$4 h and $\approx$4 days to complete the growth in CTPAB (0.01 M) and CTBAB (0.01 M) solutions, respectively. By comparison, the growth of Au nanorods in CTAB (0.1 M) and CTEAB (0.1 M) solutions takes $\approx$1 h and 5–10 h, respectively.[14,20] We also found that, in general, the nanorod growth in CTPAB and CTBAB solutions becomes slower if the surfactant concentration in the growth solution is increased (Table 1, and Supporting Information Figure S8). The nanorod growth rate is independent of the type of seeds that were used in our experiments.

Size distribution of gold nanorods: The longitudinal plasmon extinction peaks of the Au nanorods grown in both CTPAB and CTBAB solutions red-shift and become broader as the amount of the CTEAB-stabilized seed solution is reduced (Figures 1A and 2A). The tails of the longitudinal plasmon peaks finally extend beyond the detection limit of our spectrophotometer. To determine the size ranges of these Au nanorods, we carried out size measurements on two batches of Au nanorods from their low-magnification TEM images. One batch was grown in a CTPAB solution (Figure 1A, curve d), and the other batch was grown in a CTBAB solution (Figure 2A, curve e). The diameters of the Au nanorods grown in the CTPAB solution range from 4 to 11 nm, their lengths range from 25 to 150 nm, and their aspect ratios are in the range of 3 to 30. The aspect ratios of $\approx$20% of the nanorods are greater than 15. By comparison, the diameters of the Au nanorods grown in the CTBAB solution range from 3 to 10 nm, their lengths range from 15 to 350 nm, and their aspect ratios range from 2 to 70. The aspect ratios of $\approx$40% of the nanorods are greater than 15. The average aspect ratio of the nanorods grown in CTBAB solutions, 16 ± 12, is larger than that of the nanorods grown in CTPAB solutions, 10 ± 5. We further plotted the diameters of the nanorods as a function of their lengths, and the volumes as a function of their aspect ratios (Figure 4). The diameters of the Au nanorods grown in CTPAB solutions decrease as their lengths increase (Figure 4A), and the volumes of the individual nanorods decrease as the aspect ratios increase (Figure 4B). The diameters of the nanorods grown in CTBAB solutions first decrease and then slightly increase as a function of their lengths (Figure 4C). Their volumes in-

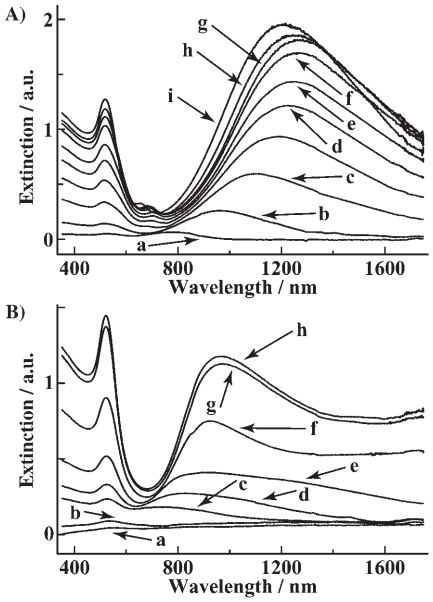

Figure 3. A) Extinction spectra of Au nanorod growth in a CTPAB solution (0.01 M) taken as a function of time after addition of the CTEAB-stabilized seed solution (0.050 mL): a) 16 min, b) 30 min, c) 45 min, d) 1.25 h, e) 1.5 h, f) 2 h, g) 2.5 h, h) 5 h, and i) 21.5 h. B) Extinction spectra of Au nanorod growth in a CTBAB solution (0.01 M) taken as a function of time after addition of the CTEAB-stabilized seed solution (0.050 mL): a) 21.5 h, b) 30 h, c) 48 h, d) 57 h, e) 68 h, f) 80 h, g) 92 h, and h) 116 h.

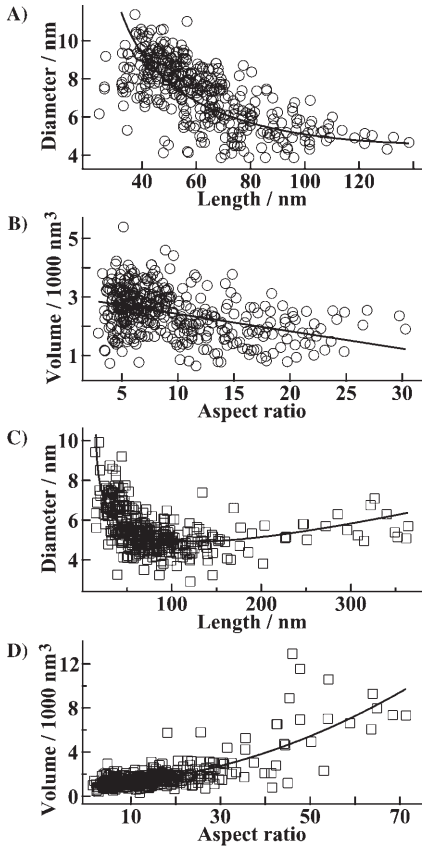

Figure 4. A) Diameter-versus-length and B) volume-versus-aspect-ratio plots of Au nanorods from the sample denoted by curve d in Figure 1A. The total number of Au nanorods measured is 395. C) Diameter-versus-length and D) volume-versus-aspect-ratio plots of Au nanorods from the sample denoted by curve e in Figure 2A. The total number of nanorods measured is 371. The solid lines are guides to the eye. Size measurements were performed on low-magnification TEM images.

crease as the aspect ratios increase (Figure 4D). The differences in the size changes between the nanorods grown in CTPAB solutions and those grown in CTBAB solutions might be due to the nanorod growth rate relative to the diffusion rate of the Au complex ions to the surfaces of growing nanorods. Because the growth of Au nanorods in CTBAB solutions is observed to be much slower than that in CTPAB solutions at the same surfactant concentration, it is probable that the nanorod growth in CTBAB solutions is comparable to or slower than the diffusion of the Au complex ions, and that the nanorod growth in CTPAB solutions is faster than the diffusion of the Au complex ions. For the diffusion-limited growth in CTPAB solutions, if more Au complex ions go to the ends of a growing nanorod and undergo reduction, fewer of them will be reduced on the side surfaces of the nanorod. Therefore, longer nanorods are generally thinner.

Crystalline structure of gold nanorods: Previous high-resolution TEM (HRTEM) imaging experiments showed that Au nanorods prepared either electrochemically or by using the seed-mediated process in the presence of Ag^+ are single-crystalline, with their side surfaces made of either the {100} or {110} facets.[20,22,23] They seem to be oriented in either the [100] or [110] direction under TEM imaging. These previous observations were made on Au nanorods with aspect ratios less than 10. It remains unclear whether the Au nanorods of larger aspect ratios are still single-crystalline and whether their crystal orientation is dependent on diameter and length.

We recorded HRTEM images of the Au nanorods grown in the same batch in a CTBAB solution (0.01 M) by using the CTEAB-stabilized seeds (Figure 2A, curve e), because the Au nanorods grown in CTBAB solutions have a larger average aspect ratio. All the nanorods that were imaged are single-crystalline. Figure 5A and B show two examples of HRTEM images of Au nanorods with large aspect ratios.

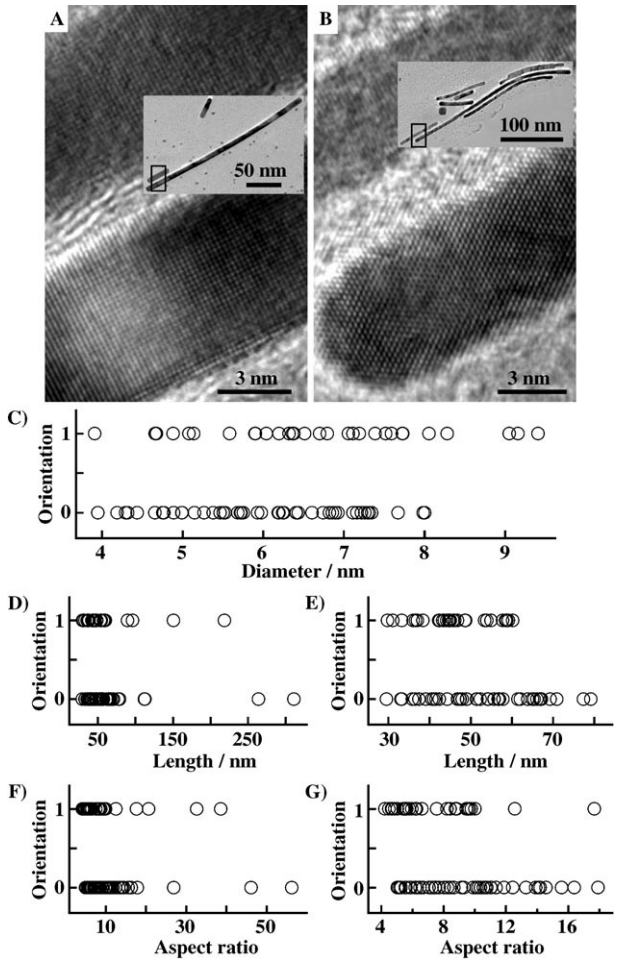

Figure 5. A) HRTEM image of two [100]-oriented Au nanorods whose aspect ratios are 4.7 and 33. Inset is the low-magnification TEM image of the nanorods. B) HRTEM image of one [110]-oriented nanorod whose aspect ratio is 43. Inset is the low-magnification TEM image of the nanorod. C) Nanorod crystal orientation versus diameter. D) Orientation versus length. E) Large-scale representation of D) for short nanorods. F) Orientation versus aspect ratio. G) Large-scale representation of F) for small-aspect-ratio nanorods. Crystal orientations of 80 Au nanorods were determined by using HRTEM. The numbers 1 and 0 on the y-axes represent the [100] and [110] orientations, respectively. The nanorods were from the sample denoted by curve e in Figure 2A.

One Au nanorod is oriented in the [100] direction and its aspect ratio is 33. The other one is oriented in the [110] direction and its aspect ratio is 43. HRTEM imaging reveals that these nanorods remain in the same crystal orientation over their entire lengths. Of the 80 nanorods that were imaged, 48 are oriented in the [110] direction, and 32 are oriented in the [100] direction. To determine the relationship between the crystal orientations and sizes, we measured the diameters and lengths of these nanorods. The numbers 1 and 0 on the y-axes were used to represent the [100] and [110] orientations, respectively. Figure 4C–G show the plots of the crystal orientation as a function of nanorod diameter, length, and aspect ratio, respectively. The crystal orientation fluctuates randomly between [100] and [110] as the diameter, length, and aspect ratio vary over broad ranges. Taking together these observations and previous HRTEM imaging results,[20,22] we believe that each Au nanorod is enclosed by both the {100} and {110} facets and its cross section is octagonal, as shown schematically in Figure 6. This is in agreement with a previous dark-field TEM imaging result,[23] showing that single-crystalline nanorods exhibit three thickness bands along the transverse direction. The two side bands are symmetrical around the central band. Such thickness variation along the transverse direction suggests clearly that the nanorod cross section is octagonal. If these nanorods are deposited onto TEM grids, the probabilities for them to be oriented in either the [100] or [110] direction are equal.

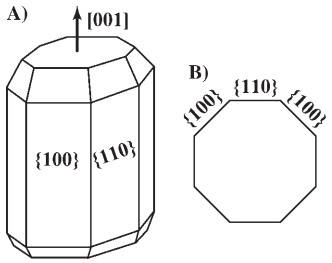

Figure 6. A) Schematic model of a single-crystalline Au nanorod. B) Cross section of the nanorod.

Comparison of nanorod-growth behavior in CTAB, CTEAB, CTPAB, and CTBAB solutions: Our experiments on the growth of Au nanorods in CTPAB and CTBAB solutions, together with previous studies with CTAB and CTEAB solutions,[14,20] allow for the exploration of nanorod-growth behavior as a function of the headgroup size of these cationic surfactants. Table 2 summarizes the results of the one-step nanorod growth in the four surfactant solutions achieved by using the seed-mediated process in the presence of $AgNO_3$. The average nanorod aspect ratio increases and the nanorod growth rate decreases as the headgroup becomes larger. Because these surfactants form micelles at the concentrations used for Au nanorod growth, their micelle properties are also included in this table. The four cationic surfactants have the same tail length. Their critical micelle concentrations and micelle aggregation numbers decrease as the size of the headgroup increases. Their fractional dissociation constants of Br^- ions increase as the headgroup size increases.

During Au nanorod growth, surfactants are adsorbed onto the surfaces of nanorods to form a bilayer.[19] The positively charged headgroups in the layer closer to the Au surface are bound to the surface through electrostatic interactions. The formation of the surfactant bilayer not only makes Au nanorods positively charged and, thus, stabilizes them in aqueous growth solutions, but also changes the growth rates at nanorod side surfaces and ends. The Au nanorods grown in the presence of $AgNO_3$ are single-crystalline. Their side surfaces are composed of both the {100} and {110} facets. The surfactant bilayer formed on the side surfaces should be more stable than that at the ends, at which there is a sharp curvature. Therefore, formation of the surfactant bilayer slows down the growth of Au nanorods at the side surfaces. It is observed clearly in our experiments that the average aspect ratio of Au nanorods increases and the nanorod growth rate decreases as the surfactant headgroup becomes larger. This observation suggests that the surfactant with a larger headgroup should form a more stable bilayer on the surfaces of Au nanorods. The formation of the more stable bilayer probably results from the reduced repulsive electrostatic interaction between the larger headgroups. The presence of the more stable bilayer reduces the overall growth rate of Au nanorods. Therefore, the growth of Au nanorods becomes slower as the surfactant headgroup becomes larger. In addition, the surfactant bilayers adsorbed onto the flat side surfaces should be more stabilized than those adsorbed at the ends having a sharp curvature. This leads to an increase in the ratio of the growth rate at the ends to that at the side surfaces. As a result, the average aspect ratios of the Au nanorods grown by using surfactants with larger headgroups become larger.

Table 2. Micellar properties of CTAB, CTEAB, CTPAB, and CTBAB and their nanorod-growth behaviors.

Surfactant	cmc [mM][a]	α[b]	N[c]	σ of Au NRs[e]	NR growth time
CTAB	0.89	$\approx$0.2	$\approx$90[d]	$<$5[f]	$\approx$1 h (0.1 M)[f]
CTEAB	0.81	0.38	80–50	$<$11[g]	5–10 h (0.1 M)[g]
CTPAB	0.56	0.49	70–40	3–30	$\approx$3 d (0.1 M)
				$>$15 (20%)[h]	$\approx$4 h (0.01 M)
CTBAB	0.24	0.66	50–30	2–70	$\approx$4 d (0.01 M)
				$>$15 (40%)[h]	

[a] Critical micelle concentration (cmc), from ref. [24]. [b] α represents the fractional ionic dissociation constant of Br^- ions from micelles, from ref. [24]. [c] N is the aggregation number of micelles, from ref. [24]. [d] From ref. [25]. [e] σ is the aspect ratio of Au nanorods (NRs). [f] From ref. [14]. [g] From ref. [20]. [h] Numbers in parentheses are typical yields of Au nanorods with aspect ratios greater than 15 if their longitudinal plasmon peaks extend significantly beyond $\approx$1800 nm.

Conclusion

We have prepared gold nanorods in high yields in aqueous CTPAB and CTBAB solutions in the presence of silver nitrate by using the one-step seed-mediated process. These nanorods are single-crystalline. Their side surfaces are enclosed by the {100} and {110} facets. They appear either [100]-oriented or [110]-oriented under TEM imaging, irrespective of their sizes. Size measurements show that the Au nanorods grown in CTPAB solutions have lengths of up to 150 nm and aspect ratios of up to 30. Those grown in CTBAB solutions have lengths of up to 350 nm and aspect ratios of up to 70. The nanorods grown in CTPAB solutions decrease slightly in volume as the aspect ratio increases, whereas those grown in CTBAB solutions increase slightly in volume as the aspect ratio increases. Our experiments on the growth of Au nanorods in CTPAB and CTBAB solutions, together with previous studies for CTAB and CTEAB solutions, indicate unambiguously that the average aspect ratios of the Au nanorods increase and the nanorod growth rates decrease as the cationic surfactant headgroup becomes larger. We believe that the increased nanorod aspect ratios and reduced growth rates are due to the more stable bilayers formed on the Au surface from the surfactants with larger headgroups.

Experimental Section

Materials and measurements: 1-Bromohexadecane, triethylamine, tripropylamine, tributylamine, CTAB, $HAuCl_4 \cdot 3H_2O$, $NaBH_4$, ascorbic acid, and $AgNO_3$ were purchased from Aldrich and were used without further purification. Acetonitrile and ethyl acetate were purchased from Lab-Scan. Deionized water with a resistivity of 18.1 $M\Omega\,cm^{-1}$ was used in the preparation of gold nanoparticle seeds and nanorods.

Extinction spectra were recorded by using a Hitachi U-3501 UV-visible/NIR spectrophotometer. Mass spectra were recorded by using a Finnigan MAT 95XL GC mass spectrometer. Low-magnification TEM images were collected by using a FEI CM120 microscope at 120 kV. HRTEM images were taken by using a TECNAI 20 ST microscope at 200 kV. For TEM characterization, an as-grown gold nanorod solution (6 mL) was centrifuged at 19000 g for 10 min. The precipitate was redispersed in deionized water (6 mL), centrifuged again at 19000 g for 10 min, and finally redispersed in deionized water (0.5 mL). The resulting Au nanorod solution (10 μL) was drop-cast onto a lacey-formvar carbon-stabilized TEM grid and allowed to dry in the open atmosphere overnight.

Synthesis of CTEAB, CTPAB, and CTBAB surfactants: CTEAB was prepared by refluxing stoichiometric amounts of 1-bromohexadecane and triethylamine in dry acetonitrile for 24 h, as described previously.[26] The volume ratio of the total reactant to the solvent was 1:2.2. The yellow two-phase mixture remaining after reflux was rotary evaporated to remove the solvent. The resulting solid product was recrystallized from ethyl acetate 1–3 times until all of the impurities were removed. CTPAB and CTBAB were prepared in a similar way by using tripropylamine and tributylamine, respectively. The purities of CTEAB, CTPAB, and CTBAB were checked by mass spectrometry: MS (ESI): *m/z* for CTEAB: 326 $[C_{22}H_{48}N]^+$; *m/z* for CTPAB: 368 $[C_{25}H_{54}N]^+$; *m/z* for CTBAB: 410 $[C_{28}H_{60}N]^+$.

Preparation of seeds: Four types of Au nanoparticle seeds were used. For a typical preparation of CTAB-stabilized seeds, an aqueous $HAuCl_4$ solution (0.125 mL, 0.01 M) was added into an aqueous CTAB solution (3.75 mL, 0.1 M) in a plastic tube. After the solution was mixed by gentle inversion, an ice-cold, freshly prepared aqueous $NaBH_4$ solution (0.3 mL, 0.01 M) was added all at once, followed by rapid inversion mixing for 2 min. CTEAB- and CTPAB-stabilized seeds were prepared according to the same procedure by using CTEAB and CTPAB at the same concentration. CTBAB-stabilized seeds were prepared by using the same procedure with CTBAB (0.01 M). The resulting seed solutions were kept at RT and were used within 2–5 h of preparation, except for the CTBAB-stabilized seed solution, which was used within 1–2 h of preparation.

Growth of gold nanorods: The growth of gold nanorods by using the seed-mediated process in aqueous cationic surfactant solutions was achieved by following the procedure reported previously.[14,21] For example, for a typical growth in CTPAB solutions using the CTEAB-stabilized seeds, multiple aliquots of a growth solution were prepared. For each aliquot, an aqueous $HAuCl_4$ solution (0.3 mL, 0.01 M) and $AgNO_3$ solution (0.045 mL, 0.01 M) were added into an aqueous CTPAB solution (7.125 mL, 0.01 M) in a plastic tube, followed by gentle inversion mixing. A freshly prepared ascorbic acid solution (0.050 mL, 0.1 M) was then added and the resulting solution was mixed. Varying volumes of the CTEAB-stabilized seed solution were finally added into each aliquot of the growth solution. The reaction mixtures were mixed by gentle inversion for 10 s and were either left undisturbed or were used for the time-dependent measurements of extinction spectra. This procedure was applied for all of the growth processes, except that different types of seeds and surfactants were used (Table 1).

Acknowledgements

This work was supported in part by the start-up funding for J.F.W. from CUHK, by the Institute of Collaborative Biotechnologies through Grant DAAD19–03-D-0004, from the USA Army Research Office, and by the USA National Science Foundation through Grant DMR 02–33728.

[1] a) J. Pérez-Juste, I. Pastoriza-Santos, L. M. Liz-Marzán, P. Mulvaney, *Coord. Chem. Rev.* **2005**, *249*, 1870–1901; b) C. J. Murphy, T. K. Sau, A. M. Gole, C. J. Orendorff, J. X. Gao, L. F. Gou, S. E. Hunyadi, T. Li, *J. Phys. Chem. B* **2005**, *109*, 13857–13870; c) L. M. Liz-Marzán, *Langmuir* **2006**, *22*, 32–41.

[2] a) S. Link, M. B. Mohamed, M. A. El-Sayed, *J. Phys. Chem. B* **1999**, *103*, 3073–3077; b) B. H. Yan, Y. Yang, Y. C. Wang, *J. Phys. Chem. B* **2003**, *107*, 9159–9159; c) A. Brioude, X. C. Jiang, M. P. Pileni, *J. Phys. Chem. B* **2005**, *109*, 13138–13142.

[3] R. Weissleder, *Nat. Biotechnol.* **2001**, *19*, 316–317.

[4] C. Sönnichsen, A. P. Alivisatos, *Nano Lett.* **2005**, *5*, 301–304.

[5] X. H. Huang, I. H. El-Sayed, W. Qian, M. A. El-Sayed, *J. Am. Chem. Soc.* **2006**, *128*, 2115–2120.

[6] a) K. Imura, T. Nagahara, H. Okamoto, *J. Phys. Chem. B* **2005**, *109*, 13214–13220; b) H. F. Wang, T. B. Huff, D. A. Zweifel, W. He, P. S. Low, A. Wei, J.-X. Cheng, *Proc. Natl. Acad. Sci. USA* **2005**, *102*, 15752–15756.

[7] a) C.-Z. Li, K. B. Male, S. Hrapovic, J. H. T. Luong, *Chem. Commun.* **2005**, 3924–3926; b) H. W. Liao, J. H. Hafner, *Chem. Mater.* **2005**, *17*, 4636–4641.

[8] P. K. Sudeep, S. T. S. Joseph, K. G. Thomas, *J. Am. Chem. Soc.* **2005**, *127*, 6516–6517.

[9] H. Takahashi, Y. Niidome, S. Yamada, *Chem. Commun.* **2005**, 2247–2249.

[10] Y.-Y. Yu, S.-S. Chang, C.-L. Lee, C. R. C. Wang, *J. Phys. Chem. B* **1997**, *101*, 6661–6664.

[11] a) F. Kim, J. H. Song, P. D. Yang, *J. Am. Chem. Soc.* **2002**, *124*, 14316–14317; b) O. R. Miranda, T. S. Ahmadi, *J. Phys. Chem. B* **2005**, *109*, 15724–15734.

[12] a) N. R. Jana, L. Gearheart, C. J. Murphy, *J. Phys. Chem. B* **2001**, *105*, 4065–4067; b) B. D. Busbee, S. O. Obare, C. J. Murphy, *Adv. Mater.* **2003**, *15*, 414–416; c) J. Pérez-Juste, L. M. Liz-Marzán, S. Carnie, D. Y. C. Chan, P. Mulvaney, *Adv. Funct. Mater.* **2004**, *14*, 571–579.

[13] B. Nikoobakht, M. A. El-Sayed, *Chem. Mater.* **2003**, *15*, 1957–1962.
[14] T. K. Sau, C. J. Murphy, *Langmuir* **2004**, *20*, 6414–6420.
[15] a) L. F. Gou, C. J. Murphy, *Chem. Mater.* **2005**, *17*, 3668–3672; b) N. R. Jana, *Small* **2005**, *1*, 875–882; c) X. C. Jiang, A. Brioude, M. P. Pileni, *Colloids Surf. A* **2006**, *277*, 201–206.
[16] J. X. Gao, C. M. Bender, C. J. Murphy, *Langmuir* **2003**, *19*, 9065–9070.
[17] a) N. R. Jana, *Chem. Commun.* **2003**, 1950–1951; b) A. Gole, C. J. Murphy, *Chem. Mater.* **2004**, *16*, 3633–3640; c) H.-Y. Wu, H.-C. Chu, T.-J. Kuo, C.-L. Kuo, M. H. Huang, *Chem. Mater.* **2005**, *17*, 6447–6451; d) H. M. Chen, H.-C. Peng, R.-S. Liu, K. Asakura, C.-L. Lee, J.-F. Lee, S.-F. Hu, *J. Phys. Chem. B* **2005**, *109*, 19553–19555.
[18] a) J. K. N. Mbindyo, B. D. Reiss, B. R. Martin, C. D. Keating, M. J. Natan, T. E. Mallouk, *Adv. Mater.* **2001**, *13*, 249–254; b) E. Dujardin, L.-B. Hsin, C. R. C. Wang, S. Mann, *Chem. Commun.* **2001**, 1264–1265; c) K. K. Caswell, J. N. Wilson, U. H. F. Bunz, C. J. Murphy, *J. Am. Chem. Soc.* **2003**, *125*, 13914–13915; d) J.-Y. Chang, H. M. Wu, H. Chen, Y.-C. Ling, W. H. Tan, *Chem. Commun.* **2005**, 1092–1094; e) A. Gole, C. J. Murphy, *Chem. Mater.* **2005**, *17*, 1325–1330.
[19] B. Nikoobakht, M. A. El-Sayed, *Langmuir* **2001**, *17*, 6368–6374.
[20] X. S. Kou, S. Z. Zhang, C.-K. Tsung, M. H. Yeung, Q. H. Shi, G. D. Stucky, L. D. Sun, J. F. Wang, C. H. Yan, *J. Phys. Chem. B* **2006**, *110*, 16377–16383.
[21] C.-K. Tsung, X. S. Kou, Q. H. Shi, J. P. Zhang, M. H. Yeung, J. F. Wang, G. D. Stucky, *J. Am. Chem. Soc.* **2006**, *128*, 5352–5353.
[22] M. Z. Liu, P. Guyot-Sionnest, *J. Phys. Chem. B* **2005**, *109*, 22192–22200.
[23] Z. L. Wang, M. B. Mohamed, S. Link, M. A. El-Sayed, *Surf. Sci.* **1999**, *440*, L809–L814.
[24] R. Bacaloglu, C. A. Bunton, F. Ortega, *J. Phys. Chem.* **1989**, *93*, 1497–1502.
[25] P. Lianos, R. Zana, *J. Colloid Interface Sci.* **1981**, *84*, 100–107.
[26] S. A. Buckingham, C. J. Garvey, G. G. Warr, *J. Phys. Chem.* **1993**, *97*, 10236–10244.

Received: August 24, 2006
Published online: December 21, 2006

